STUDY OF UTILIZING ENERGY BEAMS IN THE FABRICATION OF SEMICONDUCTOR DEVICES

S. Harrison and R. Sudbury

Ion Physics Corporation
Burlington, Massachusetts

Contract NAS8-20184

FINAL REPORT

June 1967

Prepared for:

GEORGE C. MARSHALL SPACE FLIGHT CENTER
NATIONAL AERONAUTICS AND SPACE ADMINISTRATION
HUNTSVILLE, ALABAMA

ION PHYSICS CORPORATION
A Subsidiary of High Voltage Engineering Corporation
BURLINGTON, MASSACHUSETTS

STUDY OF UTILIZING ENERGY BEAMS IN THE FABRICATION OF SEMICONDUCTOR DEVICES

S. Harrison and R. Sudbury

Ion Physics Corporation
Burlington, Massachusetts

Contract NAS8-20184

FINAL REPORT

June 1967

Prepared for:

GEORGE C. MARSHALL SPACE FLIGHT CENTER
NATIONAL AERONAUTICS AND SPACE ADMINISTRATION
HUNTSVILLE, ALABAMA

CONTRIBUTORS

The following staff members have contributed to this project:

Personnel	Position	Program Function
Dr. W.J. King	Department Manager	Program Manager
S. Harrison	Group Leader	Project Physicist
R. Sudbury	Senior Physicist	Device Studies

In addition, the following technical personnel have been highly instrumental in the development of microbeam systems and technology:

Personnel	Position	Program Function
R. Berman	Engineering Aide	Microbeam Technology
A. Boom	Engineering Aide	Acceleration Technology
P. Donaher	Technician	Electronics

ABSTRACT

The purpose of this contract has been to study and explore methods of utilizing ion implantation techniques for producing semiconductor devices without the need for complex multi-step masking and photoresist-etch processing.

By the use of proper electrostatic or electromagnetic lenses, the ion beam from an accelerator can be focused and utilized to "write" with dopant ions in semiconductors, forming electrical devices. A 16-hole mask placed in the beam path has been successfully imaged with reduced magnification by a quadrupole lens system on a substrate about 3 meters away.

During the course of the contract, a lens system and associated vacuum and electronic equipment were designed, constructed and tested. The design energy range was 50 kev to 1 Mev with the lens generally operating with 80 to 100 kev ions. The lens system is electrostatic so that focusing is independent of ion species. This capability has been demonstrated as the lens has worked equally well on phosphorus, boron, helium and sulfur ions.

Early work led to a 5 micron resolution, but the need for rapid focusing and real time monitoring was obvious. A low-power secondary electron microscope was constructed inside the target chamber which ultimately gave a 30X magnified image of the spot being implanted, on a phosphor screen. The image is derived from the secondary electrons created by the ion beam at the silicon substrate. The secondary emission microscope greatly speeded implantation experiments.

A field effect device was made by scanning a single defocused beam from one heavily implanted area to a subsequent area that was then heavily implanted. The defocused beam was utilized to fabricate a device large enough to be easily contacted with probes.

A tantalum mask with 16 rectangular holes was inserted in front of the lens system. The resulting beams implanted 0.005 x 0.007 mm rectangles at the substrate over an area approximately 1 mm square. By electrically scanning the beams, an array of 16 FET structures with apparent edge resolution of better than 5 microns was written. The beam could also be electrically scanned to form larger contact areas.

TABLE OF CONTENTS

LIST OF ILLUSTRATIONS

1. INTRODUCTION

1.1 Background

The process of ion implantation may be defined as one in which p-n junctions are fabricated in semiconductor materials by bombardment with beams of energetic dopant ions. This area is one which has assumed increasing importance in the semiconductor industry during the last few years. For this reason, a brief history of recent developments is given.

Ion implantation, as a basic process for selectively doping semiconductor materials, has been investigated in various forms for a period of greater than ten years. Unfortunately, much of the earlier work at Bell Telephone Laboratories was concerned primarily with radiation damage mechanisms rather than chemical doping effects. By the end of the fifties, these studies created the general impression in the semiconductor industry that ion implantation was a limited process dominated by damage effects. Investigations in the last six years, primarily by IPC, have shown that exactly the converse is true. Not only can radiation damage effects be readily annealed out, allowing chemical doping effects to dominate, but the implantation process, when properly applied, can be extremely flexible and well controlled as compared to the diffusion process. This has been clearly demonstrated by results on silicon solar cells.

1.2 Implantation Technique

In brief, the implantation technique at IPC has consisted of irradiation of silicon with energetic (50 kev to 400 kev) boron and/or phosphorus ions, which penetrate to controlled depths 0 to 1.3 microns below the surface of the silicon, depending on their energy. After a suitable anneal to remove radiation-induced defects and cause the ions to become substitutional impurity atoms, a distribution of a dopant concentration versus profile depth is obtained. The "profile" of this distribution may be varied within wide limits according to the time the ion beam is applied at each depth of penetration.

Although much basic work remains to be done on implantation mechanisms, the current state of knowledge is such that direct implantation may be widely used in device work. Historically, the experimental program at IPC started with solar cell development and has resulted in a presently marketed solar cell.

By using an ion implantation technology that includes masking the area not to be implanted and then sweeping the slice with an ion beam, Bipolar, FET, and MOS devices have been fabricated in silicon. At this time, quality MOS silicon devices are being fabricated under contract to Rome Air Development Center, United States Air Force.

For Group IV semiconductors, the advantages of the direct implantation process as compared to planar diffusion process may be described as increased control, low temperature processing, flexibility and ability to work through a surface passivating oxide, high degree of reproducibility and automation potential.

On wide-band-gap materials, ion implantation is potentially a solution to junction formation problems. The inability to selectively dope many materials by other methods has precluded the fabrication of useful devices except for a few special cases. Ion implantation may very well be the means of processing materials that may be called the more exotic semiconductors.

Work at IPC is presently underway on implanting wide-band-gap materials with junctions having been formed in silicon carbide, gallium arsenide and diamond.

1.3 Microbeam Program Objectives

An attractive method for implantation is the manipulation of the energetic ion beam in such a manner as to write desired devices in the semiconductor material. The beam can potentially be focused to produce edge resolution and/or spot size in the submicron range. With beam control techniques, elimination of many of the normal production steps can be accomplished.

The main problems to be overcome by the lens system design were the degrading effects of lens aberrations, residual gas scattering and neutralization, space charge, stray electromagnetic fields, vibration, electrical noise, etc.

The primary goal of this program has been a demonstration of a microbeam system for device fabrication. Studies of the apparatus required, the problems of beam control,and the several alternative modes of operation, have been carried out under this program. Device fabrication to demonstrate the feasibility of using a microbeam system has also been accomplished.

2. THE MICROBEAM SYSTEM

The schematic diagram and photograph of the overall system are shown in Figures 1 and 2. The ion beam formed from an RF source in the terminal of the 400 kv Van de Graaff accelerator is accelerated and focused by the acceleration tube, and then mass analyzed by the 90 degree magnet. The desired doping ion is transmitted and refocused by the magnet, while all others are intercepted by the walls of the magnet chamber. The analyzed beam exits from the magnet and passes through two current sensing "slits". At a given magnet setting the signal derived from the slits becomes unbalanced due to beam motion when the beam energy changes above or below the correct value for that ion species and magnetic field. The difference signal thus derived is fed back to control a corona load, terminal current leak, thus regulating the terminal voltage. As it leaves the slits the beam is isotopically pure and relatively monoenergetic with its average energy stabilized to better than 1 part in 10^4.

The beam then enters the microbeam ion optical system. The optical system consists of an "object" mask, an adjustable limiting aperture at the lens, a three-element quadrupole lens, and at the "image plane", a substrate holder. These are shown in Figure 3.

The beam, as it enters the orifice-mask, is analogous to the partially collimated light beam in a photographic slide projector. The light beam in a projector must be spread enough to illuminate the whole slide evenly and need not be collimated except for the fact that all rays which diverge too much will miss the useable lens aperture and be lost, thereby losing brightness.

In the ion optical system, the beam can pass through the beam mask at arbitrary angles also (i.e., at poor collimation), but the maximum efficiency will only be achieved if the beam does not expand to greater than the size of the maximum allowable input aperture of the ion lens.

Due to aperture dependent aberrations, the adjustable aperture must be used to remove beam components which are too far from the lens axis to be focused to the desired resolution level.

The portion of the beam which passes through the aperture then passes through the three-element quadrupole lens. This lens acts on the beam in the same manner as a set of three crossed cylindrical lenses acts on a light beam.

These lenses can be replaced by a theoretical lens pair placed at specific locations on the axis. These locations are known as the principle planes. One principle plane is where one simple single axis lens should be

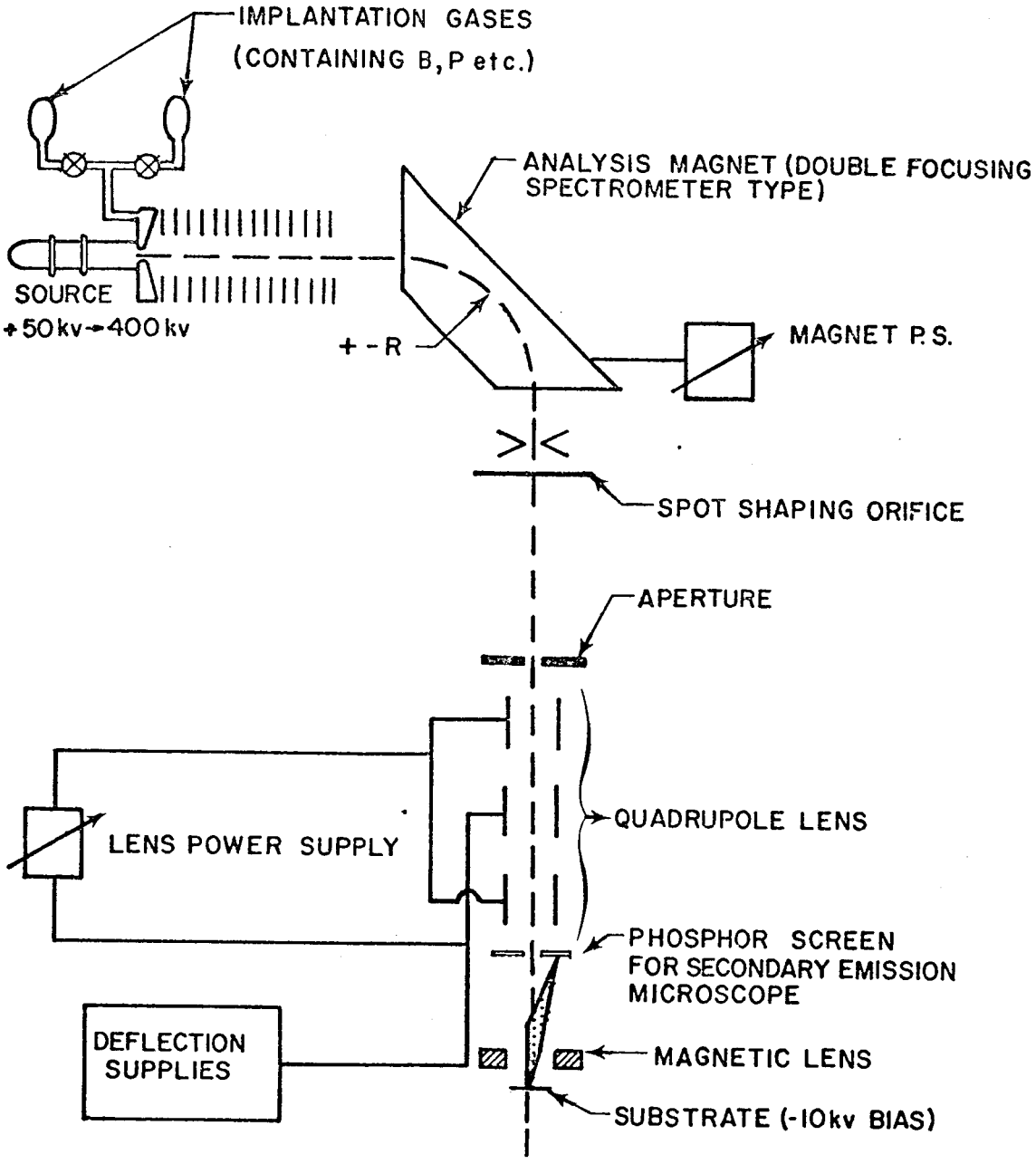

Figure 1. Microbeam System

1-2077

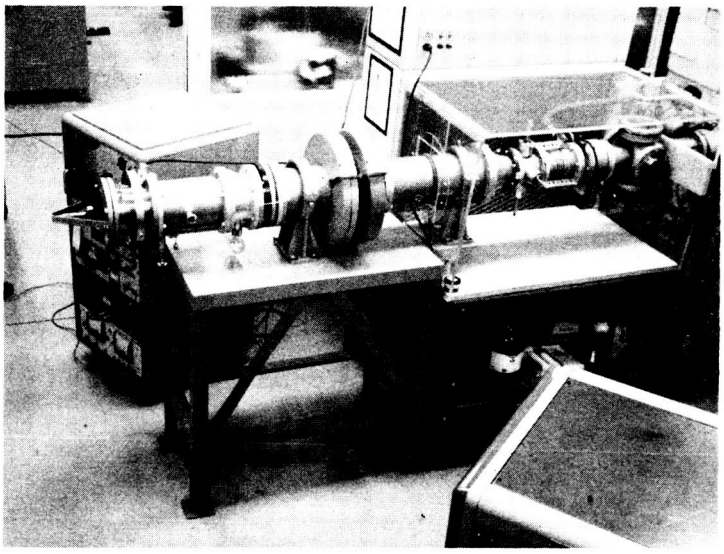

Figure 2. Microbeam Extension for
400 kev Accelerator

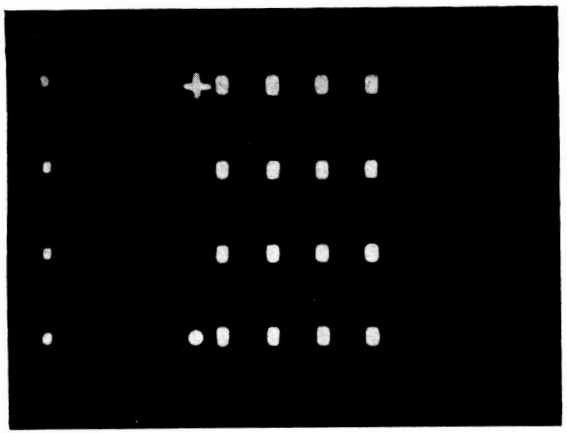

(a) Orifice Object Mask (10X)

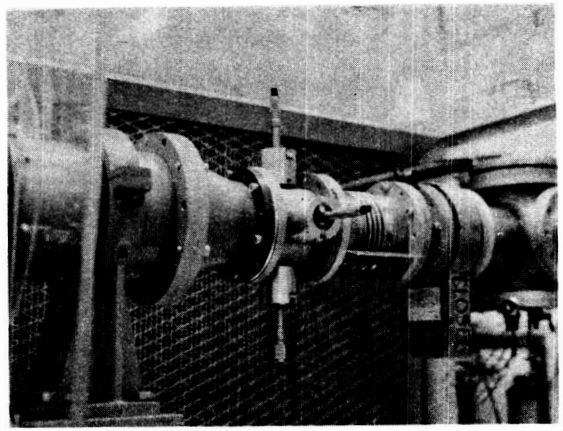

(b) Adjustable Aperature Section

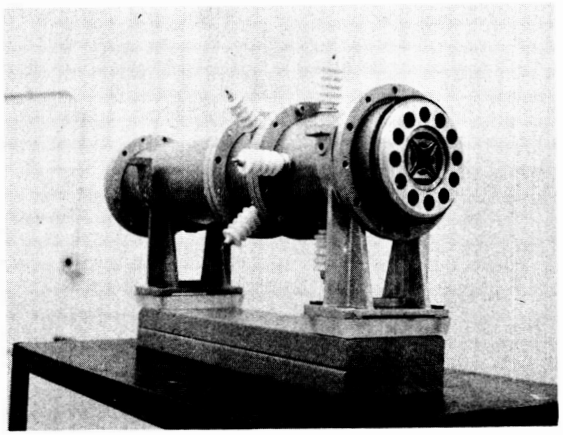

(c) Quadrupole Electrostatic Lens

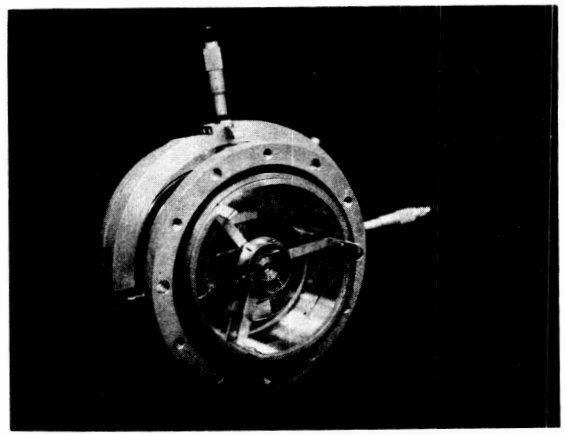

(d) Adjustable Substrate Holder with Secondary Electron Lens

Figure 3. Microbeam System Components

placed to cause X-axis focusing identical to that by the triplet and the other is where a simple lens would produce the same results on the Y-axis.

Since these theoretical lenses are at different locations and must both focus at the same location, they must be adjusted to different focal lenghts. As a result of this, the magnifications on the X- and Y-axes are different. This causes a very simple form of distortion of the image which can be removed if desired by predistortion of the object orifice. The demagnifications used in the experiments performed on this contract were about 3X and 5X. This demagnification can produce an increase in current density at the substrate which is 18 times greater than that at the orifice mask. An elongated reduced image of the orifice mask is then implanted into the substrate material to a depth determined by the ion energy.

The interaction of the ion beam with the substrate is not directly observable, but the secondary electrons caused by the interaction can be accelerated and focused onto a phosphor screen giving a magnified image of the spots being implanted.

2.1 The Acceleration System

The accelerator used on this program was converted typed PN 400 kv Van de Graaff positive ion accelerator. Figure 4 details the principles of operation and Figure 5 is a photograph of the accelerator. At the output of this accelerator is a 90 degree double focusing analysis magnet. This type of mass analyzed system seems ideal for microbeam use, although for production simpler systems could be devised for the low energy end of the spectrum.

The mass analysis of the system is desirable both for the ability to sort out the dopant which is desired at the moment and for the stability it lends to the whole feedback controlled energy stabilization system. In the future, stabilization can be improved by an order of magnitude by an ac coupled capacitive feedback system paralleling the slower magnet-corona stabilization. This will remove the higher speed transients which are not now affected, but are of importance to semiconductor work where improper operation for 1 part in 10^4 of the time can overdope the substrate over a defocused area.

The ion source used on this work was an RF type which is notable for its large ion energy spread. Better sources are available, such as the types used for isotope separators which produce more ion yield with an energy spread 10 to 100 times less than that of our RF source. The use of this type of source in the future should greatly increase the current density through the lens systems.

The operation of a Van de Graaff positive-ion accelerator involves three major steps: generation of a high dc potential; production and acceleration of a positive ion beam; measurement and regulation of the ion-beam energy.

Van de Graaff Voltage Source

1. Electric charge is sprayed, by a corona-discharge system, onto a rapidly moving insulating belt. This continuous discharge is generated from a small dc power supply, mounted inside the generator tank.
2. The belt mechanically carries the charge into a hemispherical high voltage terminal.
3. Inside the terminal, the charge is automatically transferred from the belt to the terminal. The high dc potential is established and maintained by a charge continuously flowing back to ground through a very high-resistance voltage divider.
4. The high-voltage terminal is insulated from the pressure vessel surrounding the generator by compressed nitrogen and carbon dioxide, which prevents arc-over.

By varying the flow of electric charge to the terminal, the generator voltage can be correspondingly varied. In practice, excess charge flow is utilized for the acceleration-tube load.

Positive-Ion Production and Acceleration

5. Hydrogen gas is introduced into the ion source, by a remotely controlled valve on the gas cylinder. Radio frequency power from the rf oscillator supplies the energy to ionize the gas in the ion-source bottle. A positive potential is applied to the probe, or ejection electrode, of the source, causing positive ions to be withdrawn from the plasma into the acceleration tube.
6. The positive ions are focused and accelerated by means of the electric field along the evacuated glass-and metal acceleration tube. Each metal electrode of the tube is connected to a corresponding equipotential plane whose dc potential is maintained by the voltage-divider.
7. The positive ion beam is accelerated to extremely high velocity by the potential difference between the terminal and ground ends of the acceleration tube. Because the potential is dc in nature, the particles in the beam are homogeneous in energy at any instant.

By regulating the probe potential and the gas flow to the ion source, the ion-beam current can be adjusted from the remote control station. Other gases can be introduced either by changing the gas cylinder or by remotely switching to a different gas supply.

Ion-beam Energy Measurement & Regulation

8. A rotating-vane generating voltmeter is useful either for metering the generator voltage (after suitable calibration) or for regulating the voltage within a few percent.
9. For precise measurement and control of ion-beam energy, the beam is deflected by a magnetic field whose strength is held constant by an electronically regulated dc power supply. An insulated slit system at the exit portal of the magnet permits ions of a particular mass-energy product to proceed to the experimental apparatus or nuclear target.

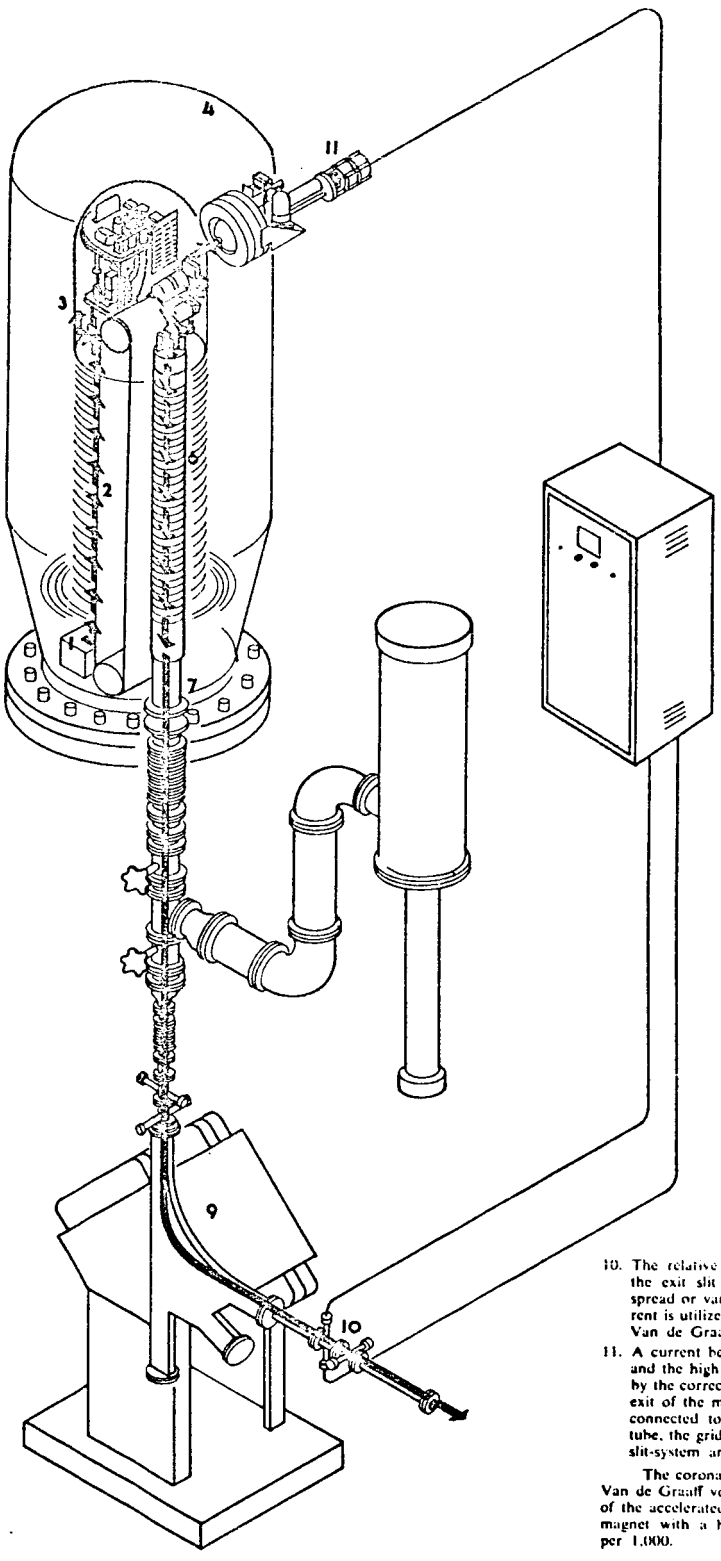

10. The relative amount of ion beam hitting the exit slit is a measure of the energy spread or variation in the beam. This current is utilized as a correcting signal to the Van de Graaff high voltage terminal.
11. A current between a set of corona points and the high voltage terminal is controlled by the correcting signal from the slit at the exit of the magnet. The corona points are connected to the plate of a high voltage tube, the grid of which is connected to the slit-system amplifier.

The corona type of control stabilizes the Van de Graaff voltage so that a large fraction of the accelerated ion beam emerges from the magnet with a homogeneity within one part per 1,000.

Figure 4. Van de Graaff Principles of Operation

1-682

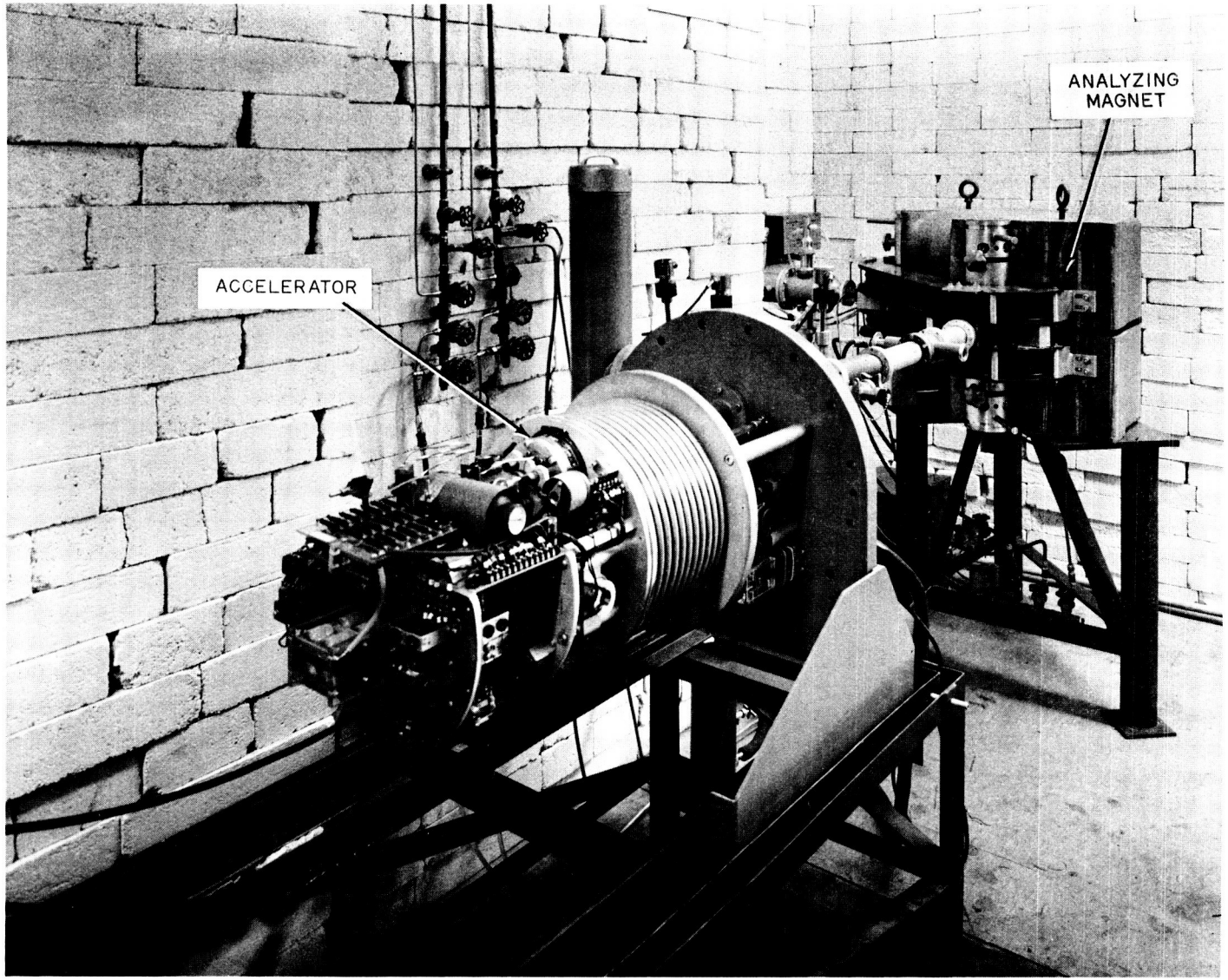

Figure 5. View of 400 kev Van de Graaff Accelerator Terminal Column and Analysis Magnet

2.2 Lens Considerations

To achieve significant demagnifications in a reasonable sized vacuum system, a short focal length is required. But to attain a maximum range of useful dopant depths, the capability of focusing energies as high as 1 Mev is desirable. A short focal length at 1 Mev would require several hundred kilovolts applied to a standard axial symmetric ion optical lens. Therefore, "strong focusing" lenses such as quadrupoles are necessary.

Electrostatic lenses were selected over magnetic, since the latter cannot produce identical field geometries at different field strengths. Due to overall saturation effects and a non-linear interdependence, magnetic lenses cannot be used by simply having the magnet current track the acceleration voltage as can be done with the voltage on an electrostatic lens. Also, a change of ion species can require a large change in magnetic field causing field distortion due to local lens metal saturation which in a magnetic lens affects registration and focal quality. With an electrostatic lens the required lens voltage is dependent only on ion energy and not on ion species and the aberrations are independent of voltage. Figure 6 shows the quadrupole lens system used for this program.

A failing of the quadrupole lens is the fact that it can focus only on one axis and defocuses on the other. Combinations must, therefore, be used with their polarities rotated such that in passing through the lens, the ion beam is focused part way through the lens and defocused the rest of the way. The net result is focusing to some extent on both axes. However, since one axis enters a focusing mode first, and during the same point, the other is defocusing, there is a lack of symmetry such that the focal lengths differ on two axes. By adjustment of the lens voltages the focal planes for the two axes can be made to correspond, but the demagnification on the two axes are different. The lens we have experimented with has had a demagnification of about 5X on one axis and about 3X on the other. This has not been a probelm in that it is fairly simple to predistort the orifice dimensions by a ratio to achieve the desired pattern after the lens. However, future lenses could probably avoid this to a great extent by having more elements such that the effect of the offending first element occurs over a smaller percentage of the overall length.

Lens electrode spacing has been adequate to minimize surface charging problems and to average out field distortion due to imperfect electrodes. However, shorter focal lengths than those used in these experiments are desirable and can be achieved by reducing the electrode spacing and lens element length.

The direction of change required in the future lens design could be to achieve a shorter image object distance by shortening the useful focal length of the lens. This can be done by shortening the elements simultaneously with reducing the electrode separation (this should not effect the magnitude of end

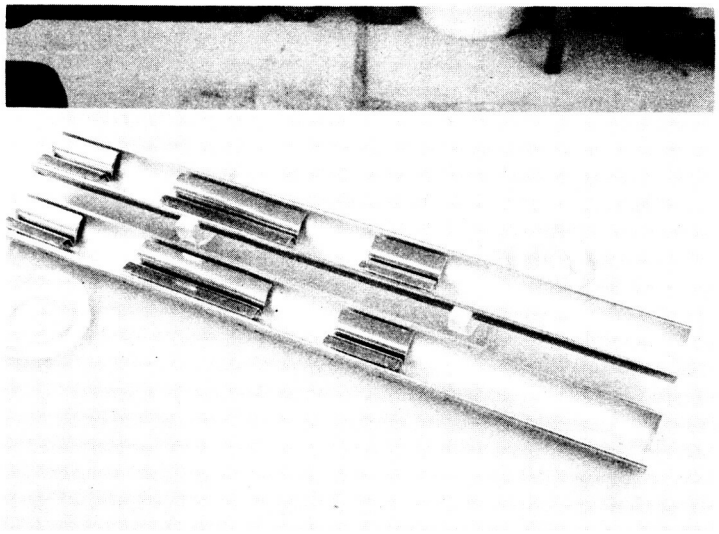

Figure 6. Quadrupole Lens Elements

effect aberration). The number of lens elements should then be increased to reduce the unequal magnification of the different lens axis.

2.3 Lens Resolution

The resolution obtained from an electrostatic lens is dependent on many design factors, and upon the elimination of spurious effects.

Perfection of the lens field is required over the range of aperture to be used, and deviations from perfection along the axis due to end effects must be minimized both in degree and percentage of lens length involved.

Electrostatic lenses suffer from total "chromatic aberrations" and the resolution is adversely affected when the variation of focal length due to variation in energy is greater than the depth of field. The depth of field in turn is inversely dependent on the size of the maximum aperture. The aperture must be large if the original beam was not sufficiently collimated at the plane where it illuminated the object mask. Even after collimation of a given beam with a perfect lens, it spreads in a manner determined by the random energy content of the beam at the time it was formed.

Because of this random spreading of the beam, the aperture of the lens must be large to pass the full beam. Thus a trade-off between current and resolution occurs. In a perfect lens the optimum aperture is the largest one which still produces sufficient resolution. Apertures greater than optimum reduce resolution due to off-axis field imperfections and focal length spread caused by chromatic aberrations.

Aberrations from imperfections of the lens field itself (which may be analogous to spherical aberration) affect resolution for a given focal length lens by the cube of the aperture, and so very rapidly become important with increasing aperture. Spherical aberration will be the major limit in the current density resolution trade-off when the input beam is relatively monoenergetic. However, the trade-off in the chromatic aberration limited case is such that increasing the aperture to obtain four times the current results in a degradation by a factor of two of resolution, whereas in the spherical aberration limited case to obtain four times the current, results in a resolution degradation of a factor of eight.

2.4 Spurious Effects on Resolution

To extrapolate from the achieved ion beam resolution of about 5 micron to about 0.2 micron which might be required for a useful production machine, some of the various potential problem areas that may have to be improved are considered.

2.4.1 Vibration

Resolution is impared by any effect which moves the beam or substrate by an amount comparable to the desired resolution. Vibration of the substrate holder by one micron will add about 1 micron of blurring to the beam edge. Vibration should be reduced by replacing the present 10 foot ion optical path with a shorter one which has a rigid unitized construction and allowed to vibrate only as a whole on relatively free mounts. Thus the vibration relationship of the orifice, lens and substrate would be greatly reduced.

2.4.2 ac Magnetic Fields

Any ac magnetic fields in the beam path cannot be allowed to deviate the beam an amount comparable to the resolution. The simple fact of putting magnetic shielding over the half of the path now unprotected will clearly reduce ac magnetic effects by more than an order of magnitude.

2.4.3 Electrostatic Fields

Electrostatic charge build-up in the system occurring on insulators or insulating films such as fingerprints or surface oxides, can charge slowly and then discharge by breakdown of the insulation, thus applying a sawtooth displacement to the beam. This displacement must also be kept small compared to the resolution desired. The surface charging of the lens elements (which up to this point has not been proved to constitute a problem) can be reduced by improved cleanliness, gold plated surfaces, and the use of a separate VacIon system which pumps the lens differentially from the rest of the system.

2.4.4 Thermal Expansion

Axial length changes due to thermal expansion must be small compared to the depth of field. These can be minimized by temperature sensing and control, using very low expansion spacers such as quartz rods, or insulation to enforce a thermal time constant greater than the implantation time, or all of these.

2.4.5 Power Supply Regulation

The ion beam used in this work is mass analyzed such that if there were an energy variation, the beam would not follow the same path and would not enter the lens; therefore the variation appears simply as a variation in current. However, the analysis system is presently designed such that a variation in magnetic field would automatically cause a change in beam energy to

maintain the beam through the system. Therefore, to maintain the beam energy, the magnetic field must be held constant. Recent tests on the system have shown the magnetic current to be stable to ± 2 parts in 10^4 over several minutes, which although probably adequate for future use, could be improved if necessary. The lens voltage power supply must also be well regulated. Presently, the various voltages are supplied by a divider network on the output of a well regulated commercial supply and filtered against pickup by a network at the electrodes. Future versions could easily have their regulation improved by the desired factor of 25 by a feedback network utilizing a portion of the voltage sensed at the lens electrodes.

2.5 Optimization of Current Density

The current density through the lens is proportional to the area of the limiting aperture in the lens. The dimensions of this aperture are related to the cube root of the resolution if the lens is "spherical aberration" limited. It is therefore, necessary to minimize "spherical" and other aperture dependent aberrations. End effects and electrode imperfections will produce aperture dependent aberrations. End effects can be reduced by designing the lens to have a greater electrode length to separation ratio, or by artificial field enforcement techniques. Electrodes can be machined more accurately than those used, and mounted with greater precision.

With these improvements, the aberration coefficient should be reduced, increasing the allowable aperture and therefore the current density at the target.

Uniformity of current density over the input orifice-mask can be achieved by scanning; however, this would result in loss of beam during the time the beam is over a closed portion of the mask. Variable rate scanning should therefore be used scanning slowly over the open areas and at least ten times as fast over the close portions.

Current density is also proportional to the yield of ions of the desired species from the source times the reciprocal of the source energy spread. Sources of better characteristics than those of the RF ion source used in these experiments are available and should increase the output current density by an order of magnitude.

2.6 Input Beam Conditioning

The ion optical system should be a rigid entity and should operate such that a beam entering its entrance orifice will automatically pass through the system on axis. This can be done by feedback controlled beam conditioning equipment in the input portion of the lens. Beam alignment and lens

vibration problems are thus minimized. The input beam must uniformly illuminate the beam defining orifices if an array is to be used. Since the accelerator output beam spot cannot easily be made sufficiently uniform to evenly illuminate an array and since even if it could, most of it would not pass through the holes of the array, it is more desirable to use a scanned beam.

The input beam can be scanned over the orifice array in a controlled rate manner such that the beam moves ten to one hundred times faster when it is not touching an orifice than when it is. In this manner, uniformity and beam efficiency are simultaneously achieved. The electronics involved to do this can incorporate a CRT, mask and photocell. The CRT scan will be driven by the beam scan signal and the CRT mask can be generated by first using ion beam sensing to unblank the CRT. This produces the corresponding dot pattern on the CRT which can be traced slightly enlarged, for the mask which is then used as the companion to that beam mask. The CRT can then be operated normally to follow the beam such that when the spot on the CRT comes under a hole in the mask, the photocell senses it and the signal triggers the scanner to reduce its scan rate until the spot again disappears behind the mask.

2.7 Beam Steering (Writing)

Beam steering is impractical in the short focal space beyond the lens, and undesirable before the lens because it would deviate the beam from the center of the lens. A practical compromise has proven to be steering with the lens elements themselves, causing only minor motion of the beam while in the lens. The steering voltages have been manually adjusted, but for practical use, should be electronically controlled to write uniform doping by scanning at a constant but adjustable rate. When used to "write" with, the start and finish locations of each line can be preselected and then the scan released by a button. This would allow each portion of the circuit to have its doping level set independently. This technique would be very useful for writing experimental circuits.

A more production-oriented technique would be to simultaneously scan the beam of a CRT with the signal scanning the bundle of ion beams. On the face of the CRT would be a mask the shape of the desired device and a photo-cell sensing light through the mask would control the blanking of the ion beam.

A more sophisticated production technique would have a complete voltage versus time program for X, Y, blanking and energy controlled by tape.

2.8 Secondary Emission Microscope

During preliminary implantations, exposures were made at many slightly different focuses to guarantee achieving at least one correctly focused

implant. The problems of this technique (i.e., the required accuracy of substrate positioning, lens voltage and accelerator voltage) became more cumbersome as the achieved resolution improved. Immediate feedback of the quality of the focus to the operator became mandatory. As a result the use of a secondary emission microscope (SEM) appeared to be the solution. A magnetic lens was used to focus the secondary electrons generated at the site of the ion impact on the substrate. It was designed around ceramic magnets to avoid the problems of vacuum feedthroughs, power dissipation, supply regulation and outgassing. Initial experiments proved that adequate brightness was readily achieved with reasonable magnification, even though the beam current was only 10^{-11} amperes.

Further refinement of the SEM resulted in a magnification of 30X over a resolved useful area of 1 mm^2 of the substrate. The resolution of the microscope has been sufficient to allow focusing of the ion beam to a resolution of about 5 microns. However, surface topology of samples have been observed to be even more highly resolved, indicating the resolution limit of the SEM to be less than 5 microns in the form it exists at the present time. It is, therefore, reasonable to expect that with the insertion of an aperture stop, the resolution of the magnetic lens can be readily improved to the submicron range. Figure 7 is a photograph of the SEM in operation with part of the image beyond its undistorted field of view.

2.9 Measurement Equipment

In addition to the normal Van de Graaff equipment used for monitoring the accelerator, a Non-Linear System XI digital voltmeter has been used to measure lens voltages and to record magnet current when used with a Leeds and Northrop tenth ohm precision resistor. By these measurements, the repeatability of the microbeam focus could be controlled. Current measurements were made using a Keithley Model 413A log scale micro-microammeter. This instrument was used to measure current at the substrate holder and facilitated corrections necessary for proper alignment as the currents varied from 10^{-7} to 10^{-12} as a result of minor adjustments.

The secondary current must be eliminated from the total current measurement to allow an accurate measure of ion beam current. At present, the secondary microscope power supply must also be disconnected when the measurement is made. Addition of an insulating union and operating the power supply from a low leakage transformer are required for accurate measurement of beam currents excluding secondary currents.

2.10 Vacuum Equipment

The vacuum system used on this machine consists of two 4 inch mercury diffusion pumps, one at the accelerator and the other at the output

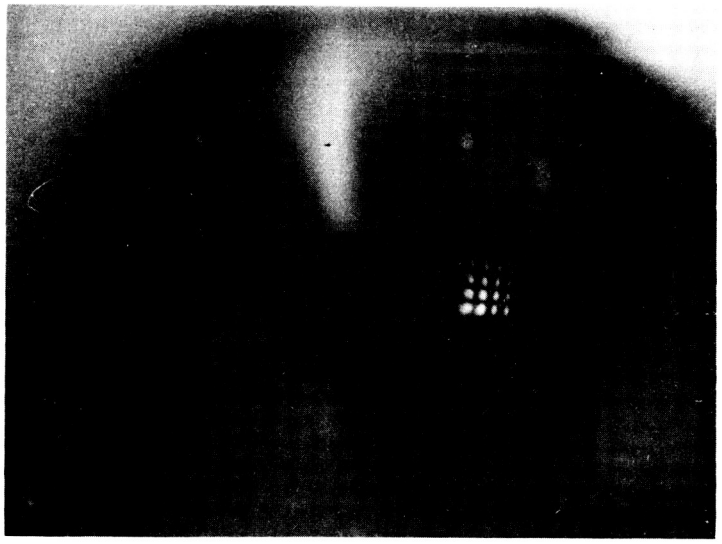

Figure 7. Photograph Through Viewing Port, of Secondary Emission Microscope Image Used for Focusing of Array During Implant in 1 Square mm of Silicon

side of the magnet. Tests have shown the pressure in the lens to be 10 times that near the second pump, and so operating pressures at the target region of 5×10^{-5} are not uncommon. This level of vacuum has been acceptable for the lens tests so far, however, better vacuum is desired due to the requirement of semiconductor implantation that the scattered background level be as small as 1 part in 10^4 under some circumstances (e.g., emitter implants). Because of the cleanliness requirements of the lens electrodes, a VacIon system pumping the lens and substrate region differentially from the rest of the system is recommended if sufficient magnetic shielding of the pump is accomplished. Pressures three orders of magnitude better could then be achieved.

3. DEVICE FABRICATION

Work on device fabrication has been performed under this contract to demonstrate the ability to "write" electrical devices with a highly resolved ion beam. This section details the parameters of the microbeam system as it relates to device fabrication. Diodes and FET devices were made by implantation on unmasked silicon slices by use of the lens system. The lens and associated equipment described in other sections of this report, as well as registration and contacting problems, place limits on the device fabrication technique. Conversely, improvements in the capabilities of the microbeam equipment should result in higher quality devices. No attempt was made to optimize the device characteristics, since the present system is adequate for manufacture of simple devices for research.

Beginning with a silicon slice, a typical fabrication process includes sputtering of a surface oxide, placing into the microbeam equipment, achieving vacuum, implanting of impurity ions as required, removing the slice from the system, annealing and contacting.

Present limitations on the process are the registration system and resolution. Resolution is approximately 5 microns. Registration requires a physical surface change of mark to be viewed on the SEM screen during implantation or use of the damaged area viewable after implanting to create a registration mark prior to annealing. Available energy, source ions, beam current and useful field area of the lens also must be considered ultimately limiting in device fabrication.

3.1 Impurity Ions

The presently available sources provide both N (phosphorus) and P (boron) doping for Group IV compounds. Other sources are available and it does not appear that ion source will be a limiting factor. The ability to use impurity sources other than those for which a diffusion technology is possible is an advantage in ion implantation.

As discussed in the lens section, the lens is electrostatic and choice of ions does not affect lens operation.

The need to switch from one ion to another quickly during a single run is obvious and while the present equipment does not have this capability modification should be accomplished without significant difficulty. All device work on this contract was done with phosphorus as the impurity ion even though other ions were implanted at various times.

The use of several n- or p-type impurities on a single slice could be accomplished and the advantages of using devices or elements fabricated from different impurities of the same type in a single integrated circuit needs to be explored.

3.2 Range Energy

Typical examples of engineering junction depth curves are shown in Figures 8 and 9. A combination of theoretical data of range energy and experimental junction depth data provide a substantial beckground of information for device design. The curves presented are only intended to be typical and the junction depth scale would be a function of impurity level in the base material.

Figure 10 shows a section of a microbeam junction implanted with P^{31} into 10 Ω cm silicon. Using the interferometric technique of Bond and Smith[1] and the junction delineation with HF according to P. J. Whoriskey[2] the computation of junction depth (d) is:

$$d = \Delta n \times \tau/2 = \Delta n \times 0.254 \cong 0.45 \text{ microns}$$

where n = number of fringes. The surface oxide was approximately 1000 angstroms and the result is in agreement with other IPC data.

Other junction sections indicated shallow junctions compared to the predicted results. Insufficient experiments have been performed to explain the shallow junction, however, very high current densities may have caused damage levels so high that additional annealing is required.

In addition to solar cells, junction unipolar and bipolar devices have been fabricated by ion implantation with energies less than 200 kev and 300 kev respectively.

An additional benefit of the range energy relationship is that a wide range of impurity profiles can be obtained by varying the energy during the implantation. Using microbeam techniques different depth-density profiles can be easily made at different locations on the slice. This advantage allows the ability to create such effects as a burried doped layer. It is expected that continuing experimentation will refine the data on range energy providing greater control on doping profile by ion implantation with a flexibility not offered by alloying or diffusion techniques. Device design should be considered with the capability of varying impurity profile. An example would be the ability to control the voltage capacitance relationship of a diode C vs $V^{1/n}$ over a range of n.

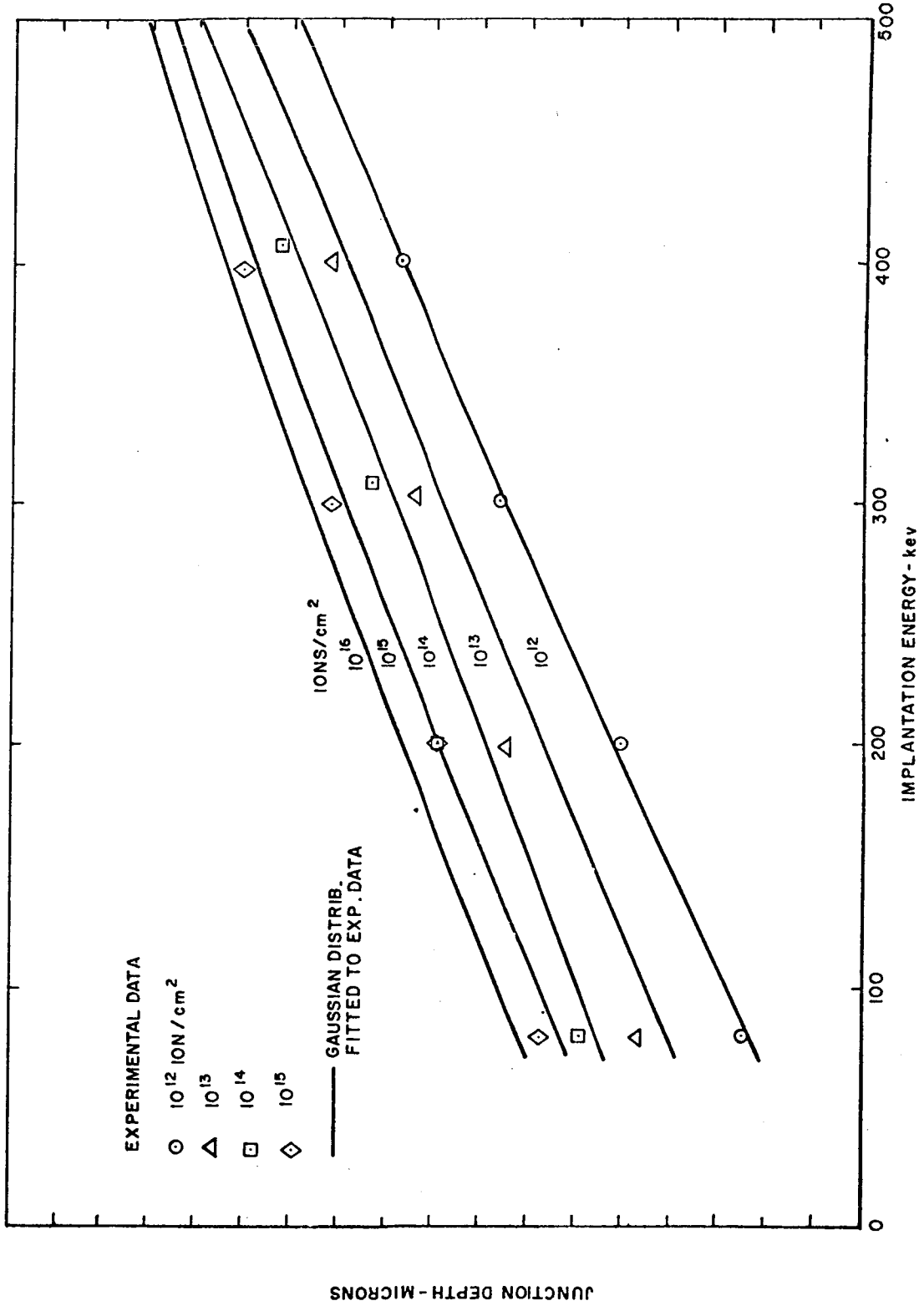

Figure 8. Junction Depth Versus Implanted Energy B^{11}

1-2076

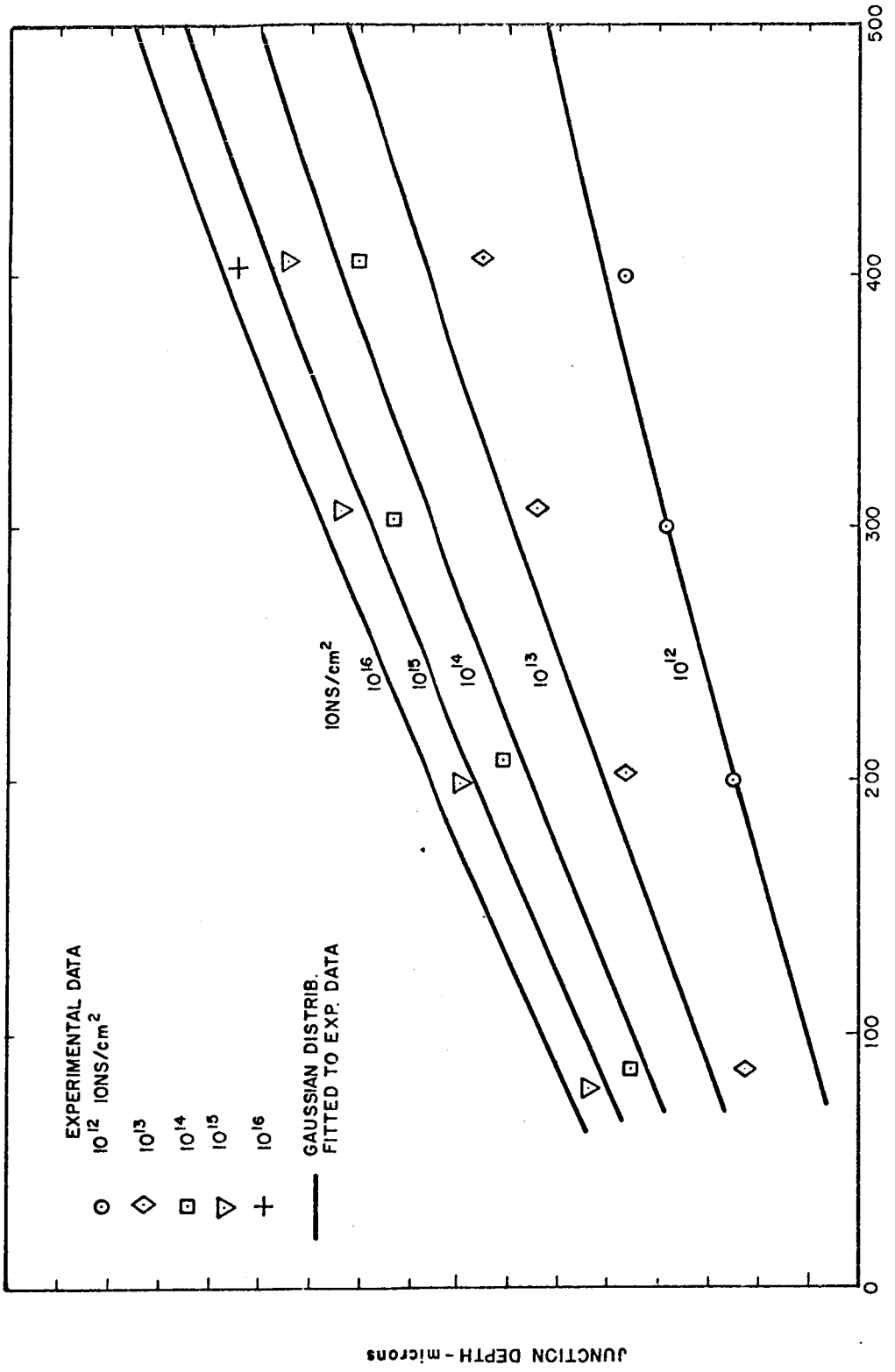

Figure 9. Junction Depth Versus Implanted Energy P^{31}

1-2075

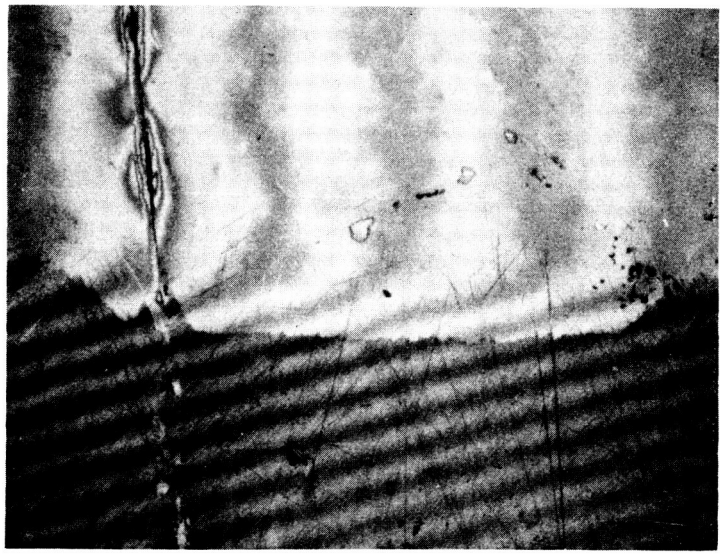

Figure 10. Implanted Area With Interference Pattern

The capability to maintain focus and registration while varying the energy are definite requirements for device work, but coupling lens voltage to accelerator voltage should be a relatively simple engineering problem.

On the experimental implantations, the beam current utilized was only a small fraction of that available at the orifice mask. For a specific application it would be expected that the percent of the current utilized through the orifice could be greatly increased. This will tend to compensate for any loss due to aperture size reduction related to lens resolution improvement.

3.3 Beam Current

The carrier concentration is a direct function of beam current and time indicating that the largest ion beam current possible is desired to reduce writing time.

In the present system, the current to the target slice is measured at the beginning and end of the implantation time. No provision has been made for the elimination of secondary electron current from the measurement, but previous work at this energy level of primary ions on silicon indicates that secondary current may account for 90% of the measured current.

The leakage through the power transformer of the electron microscope bias is significant when the current levels to be measured are in the order of magnitude 10^{-9} amp. Leakage across insulating vacuum sections must also be minimized. Measurements are now made with the secondary electron microscope (SEM) bias removed which eliminates the leakage problem due to the power supply. Removal of the SEM bias supply does affect the lens focus and it is considered desirable to continuously monitor current under normal implantation with the secondary electron microscope operating.

It is believed that beam currents of several nanoamps on areas of approximately 35×10^{-6} cm^2 or 57 microamp/cm^2 have been utilized and that significantly larger current density can be obtained by focusing and alignment of the accelerator.

Current density in the range of 100 microamp/cm^2 on areas less than 10 micron in diameter are considered practical to obtain.

Accurate current measurements are necessary for device work. This will require careful elimination of the secondary electron current and leakage currents. It may be necessary to accurately measure currents less than 10^{-9} amp when beam size is small and resolution high. The accuracy required on concentration level should not be limited by the current measurement. Accuracy of concentration is also determined by a factor such as range energy profile and percentage of impurities that occupy lattice sites after annealing. A current time measurement accuracy of $\pm$ 3% is considered sufficient.

3.4 Impurity Concentration and Profile

From range energy studies the impurity concentration can be defined in terms of the current per unit area and the time of the implantation. For 100 kev phosphorus ions, the equation for concentration is:

$$C = jt\,(10^{17})/cm^3$$

where jt is expressed in microamp sec/cm^2.

The constant term varies with energy and will require modification for higher impurity concentration where the percentage of impurities occupying lattice sites is less. For most device applications the higher impurity level will not be necessary, but during this program high levels were used so that the implanted area could be visually observed on the slice.

An orifice mask with sixteen holes, as shown in Figure 3(a), was used to demonstrate the ability to simultaneously write many devices. The beam did not illuminate the orifice mask uniformly resulting in variations in beam current densities on the sixteen implanted areas. While even illumination of the mask should easily be obtained in the future, it is presently a problem. Coupled with the unknown secondary electron current, as discussed in the beam current section, the possible range of impurity concentration may vary by a factor 10^2 around the calculated value. Assuming uniform illumination, with a secondary current 10 times primary current and the beam evenly illuminating all sixteen holes in the orifice mask for a 20 minute run at 50×10^{-9} amp, measured, the concentration would have been roughly 10^{21}/cm. Assuming only the three brightest holes were passing current, the concentration would be $6 \times 10^{21}/cm^3$. The area of a single implanted region was estimated to be 35×10^{-6} cm^2. As mentioned, the estimates of impurity in sites should be reduced at this high a concentration, but no modification has been made.

For normal device work, the desired impurity concentration might be assumed at $10^{18}/cm^3$. With the beam focused to utilize the beam current available, ion currents as high as a tenth of a nanoamp might be critically focused on to a 10 micron diameter spot. With these improvements it is reasonable to anticipate implantation times in the order of seconds for devices.

3.5 Ion Beam Size and Resolution

The present resolution of the microbeam system has been adequate for the manufacture of simple devices. Several related effects are involved in the effective resilution of the system. This section is a discussion of the effects and not a means of improving resolution. The dimension perpendicular or lateral to the beam is the direction of concern.

The resolution normally referred to in semiconductor literature is for the photographic process in masking. It is appropriate to define a resolution term for the microbeam technology.

Lateral resolution may be defined as the distance over which the implanted impurity level drops from 90% of its maximum value to 10%. This definition has been used because it is relatively easy to be determined by onserving the surface of heavily implanted material. The knowledge gained by observing the color change on the surface over implantations varying by a factor or 10 in time can be used to estimate the resolution of the implanted spots. This scheme was used as the means of describing our microbeam resolution.

It should be noted that this definition does not take into account the actual beam size. The area implanted to 90% of maximum level might be substantially different from the beam cross-sectional area calculated from the demagnification (obtained from spot spacing, not size) and the orifice hole size. This can be caused by relative movement of mechanical or electrical origin between the beam and substrate or lack of focus. Steps can be taken to reduce the variation and obtain greater control than with present day diffusion technology. The focus is now based on the qualitative observation of the image on the secondary emission phosphor screen.

The difference between the calculated size and actual size of the implant could be an increase or a decrease. A simple vibration, as shown in Figure 11, would result in the impurity level being only 1/2 of its maximum value at the width of the beam. Slight variation in focus voltage could produce a similar result. On device implants, contraction expansion in the lateral dimension has been observed. As the shape of the implant was preserved, it is reasonable to assume the change in current density over the implant area was small and, therefore, was not responsible for the reduction. Unfortunately, the corners of the mask were not sharp, making it difficult to determine if varying focus is a primary cause. No preferred axis was detected in the shape of the implanted area which indicates the limiting factor is probably not mechanical vibration. The actual demagnification was obtained by comparing spacing of the centers of the implanted rows and columns in the four by four array.

For device work, detailed knowledge of the doping profile along the lateral edge of the implanted region is required. Any variation of the implanted area from the calculated beam size must also be accounted for in the device design. The actual junction location could then be determined from substrate and implanted impurity concentrations.

Another factor needs to be defined that expresses the ability to reproduce with the microbeam system, the location and size of an implant. This would be a measure of the stability of the lens system. No experiment has been directed at determining this factor to date, but this is strictly an engineering problem. In implanting one dopant ion over another implanted region with

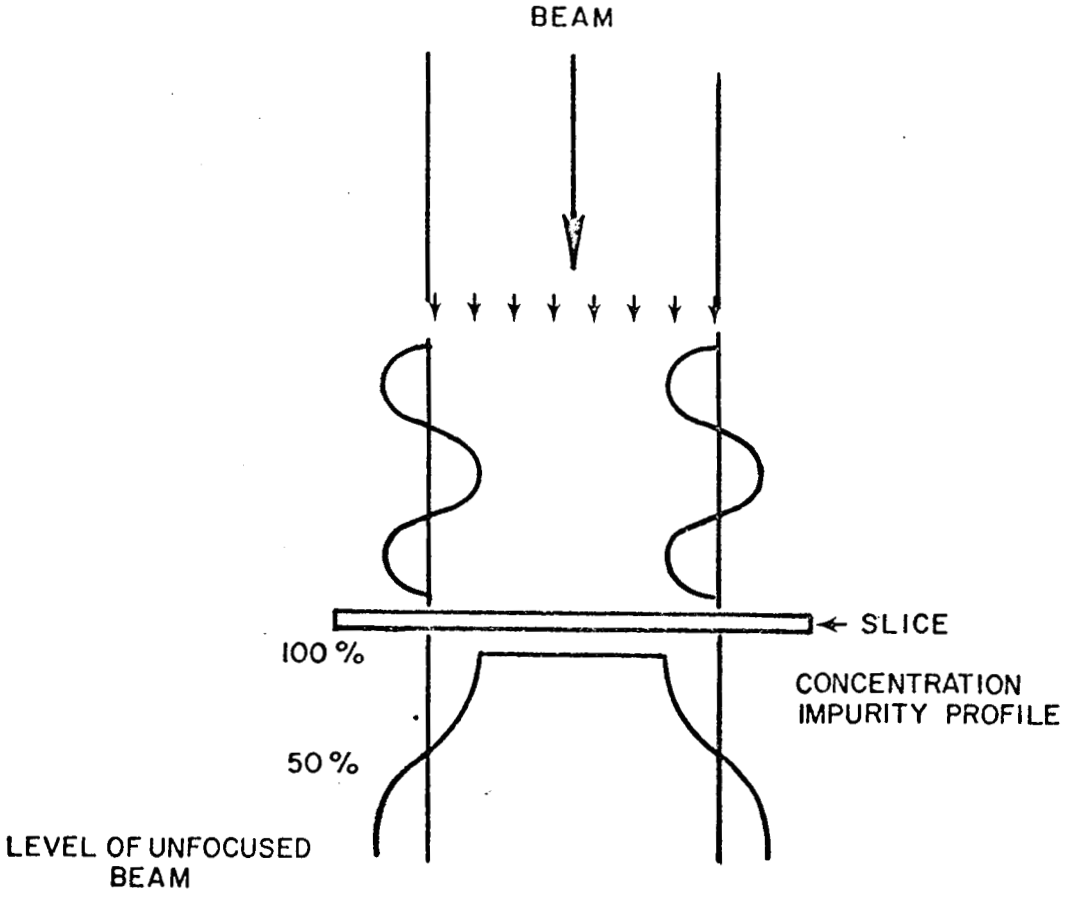

Figure 11. Effect of Vibration on Resolution

microbeam such as for a bipolar device, this will be an important term. Clearly, this stability must be measured and improved as required.

3.6 Annealing

Vacancy-impurity pairs caused by ion bombardment when present in large numbers are equivalent to a disordered crystal structure. Diffraction pictures of implanted crystals indicate low perfection, and carrier mobility is reduced through scattering effects prior to annealing. However, the ion created vacancy-impurity pairs may be annealed out at temperatures lower than those used in diffusion processing. The dominant centers in Si have been shown to anneal out below 400°C. In addition to annealing out radiation damage the dopant ion must be caused to transfer from the point where it stops to a substitutional lattice position; this requires annealing at temperatures of 400°C to 700°C.

One important result of annealing studies indicates that implanted ions are readily transferred to substitutional positions, indicating that anneals on the order of minutes are adequate.

On the device work during this program the material was typically annealed at 700°C for 20 minutes. Other work at IPC has shown this to be adequate for phosphorus implants in silicon. The annealing was carried out in an annealing furnace after the implanted material had been removed from the microbeam system.

Incorporation of an annealing step into a complete microbeam processing system could be accomplished if required.

3.7 Registration

To date, registration has been accomplished by heavily implanting the slice so that a change in the surface is visible. Then prior to annealing a mask is aligned over the visible implants. This is done prior to annealing because the visibility of the implanted area decreases significantly during the anneal.

Cerium oxide and titanium oxide coated silicon slices were used because the change in the surface is easily visible and provides contrast even when coated with photoresist. This system has the disadvantage that at lower than 10^{17} or 10^{18} implants the area may not be significantly visible to allow alignment and alignment by this method is not practical after annealing.

Attempts have been made at alignment using the secondary emission microscope by establishing a "bench mark" on the slice prior to insertion in the system then hunting with the beam across the slice to find where

the "bench mark" is located. For the experiment, slices were prepared with strips of quarts, cerium oxide, titanium oxide, and aluminum oxide. The results were inconclusive. While the edge of the strip could be detected the secondary emission characteristics were not sufficiently different to make alignment easy.

While not successfully used yet, the method of establishing a reference point before implanting is still a possible solution. Another method would be to use a beam during implantation to create a reference mask. The latter method could be coupled with a scheme for having the beam create its own contact mask.

The beam may be used to expose a high resolution film plate from which a contact mask could be fabricated. A registration mark would be included keyed to a spot on the slice. This method was experimented with as a means of fabricating a contact mark and the system adapted for insertion of a high resolution plate where the silicon is normally mounted. Poor contrast prevented the mask from being used, but the method seems practical and additional work indicated.

3.8 Contacts and Interconnections

The microbeam system could be used to "write" low resistance paths in the silicon substrate for interconnection. For simple circuits this may be done but it is anticipated that in an increasingly complicated circuit several layer of interconnecting wiring will be required.

This indicates the use of masking for metalized overlays of interconnecting paths and at the same time create contact pads. The "writing" of very low resistance paths unless it entirely eliminates the need for masking does not seem practical due to the impurity level and area required.

However, the contact mask does not need to have the resolution required for device geometry. An example is shown in Figure 12. After implanting through a thin oxide layer, holes are sputtered open through the oxide with a low energy beam where contact pads are required. A metal film is deposited and the contact pattern is superimposed by the use of photoresist. Selective etching of the deposited metal layer is than accomplished to form interconnecting layers.

3.9 Devices

A number of attempts were carried out to implant to make devices. Using a 16 hole orifice mask an array of 16 implanted spots approximately 50 by 70 microns were created. Figure 13 shows the titanium oxide coated silicon

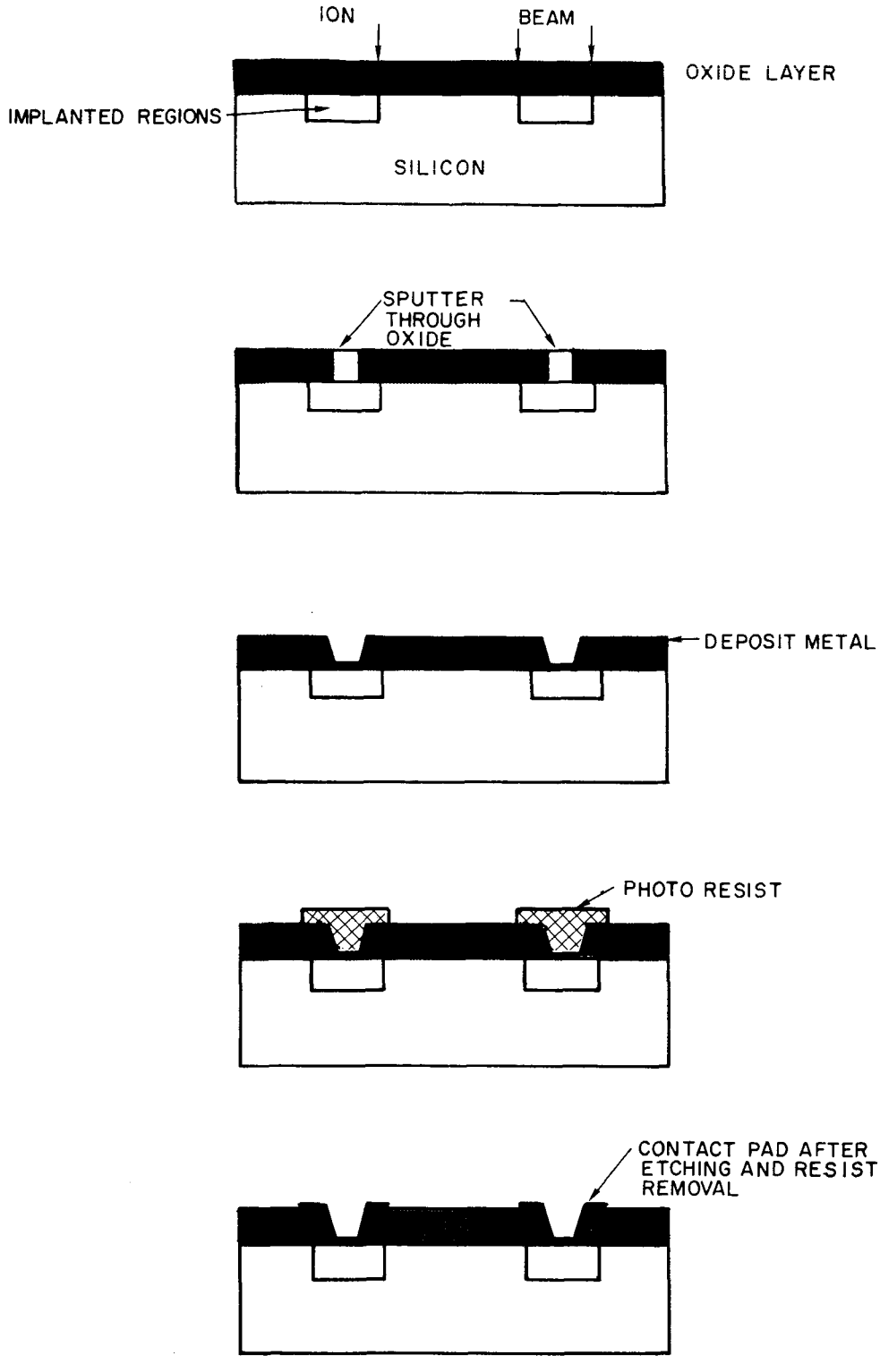

Figure 12. Contact Sequence for Microbeam Implanted Diodes

1-2079

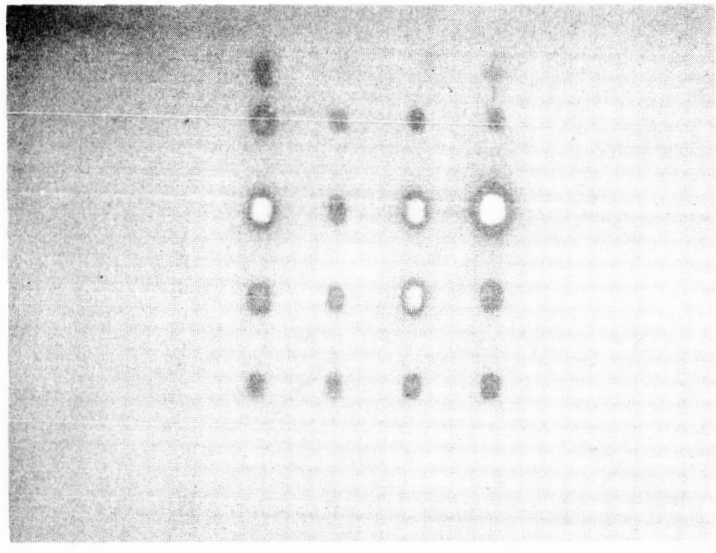

Figure 13. Silicon Slice with Implanted 16 Diode Array Prior to Annealing (38X)

slice after implanting. These areas could be identified electrically by probing the slice after annealing.

Silicon slices of p-type with impurity concentration of $1 \times 10^{15}/cm^3$ were used as base material. The ion beam was P^{31} with 80 or 100 kev energy. The energy was constant during a run and therefore, the profile was not varied. No attempt was made to optimize device parameters. The implantations were very heavy to facilitate registration.

The processing steps after implant were:

(1) etch the unimplanted titanium oxide off,
(2) annealing at 700°C for 20 minutes,
(3) vacuum deposits 1000 Å Al on the back,
(4) fire in the back contact at 600°C for 1-1/2 minutes,
(5) mask and etch the titanium oxide off the implanted area,
(6) remask and sputter nickel contacts on the front.

It would be desirable to remove the oxide from only the implanted area but the material was significantly more resistant to etching after implantation and a technique to selectively remove it prior to the photoresist lifting was not developed. Attempts to remask and open holes in the resist prior to sputtering the nickel contact were not successful. The sputter contact was not adhering well indicating a film on the surface.

Figure 14 shows one of the diodes. This curve was obtained by probing the implanted area after most of the nickel had been removed and the forward resistance was very sensitive to location. Additional diode curves taken on a larger implanted area with sputtered contacts is shown in Figure 15. This junction was sectioned and is shown in Figure 9.

The beam was moved electrically to "write" a channel for an FET device as shown in Figure 16. Figure 17 shows the implanted slice, with an array of 16 devices. Probing has indicated diodes and a channel.

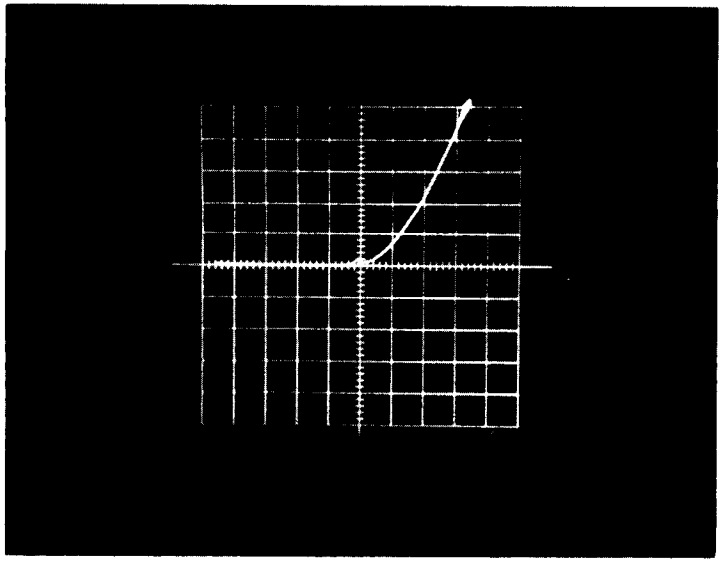

Vertical Scale: 1 ma/division

Horizontal Scale: Forward 2 v/division
Reverse 20 v/division

Figure 14. Diode Characteristic of Microbeam Implanted Junction

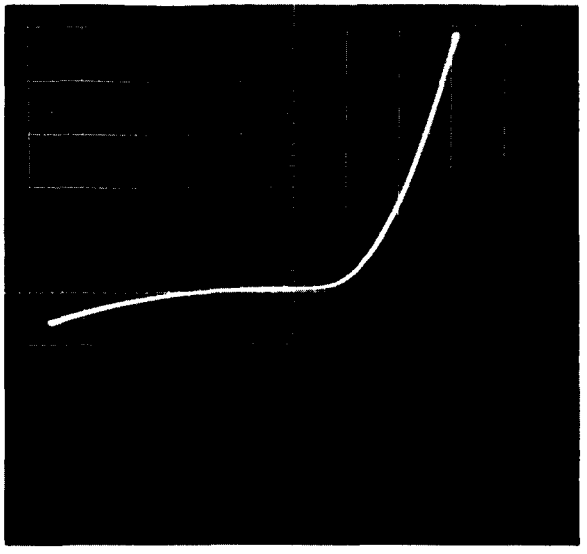

(a)

Scale:

Vertical: 1 ma/division
Horizontal: Forward 0.5 v/division
Reverse 5 v/division

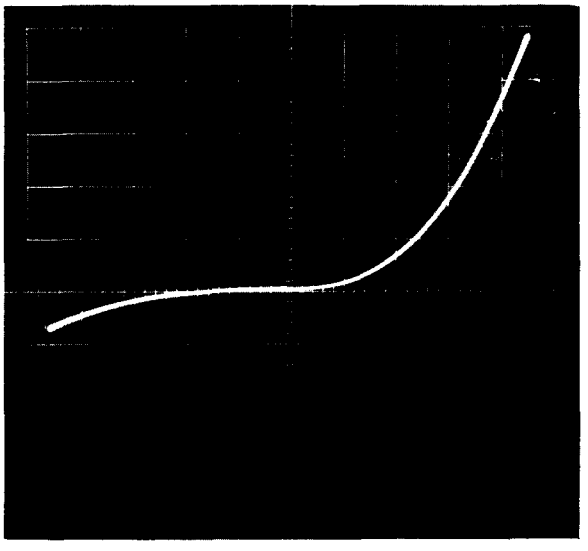

(b)

Figure 15. Large Area Maskless Diode Implants

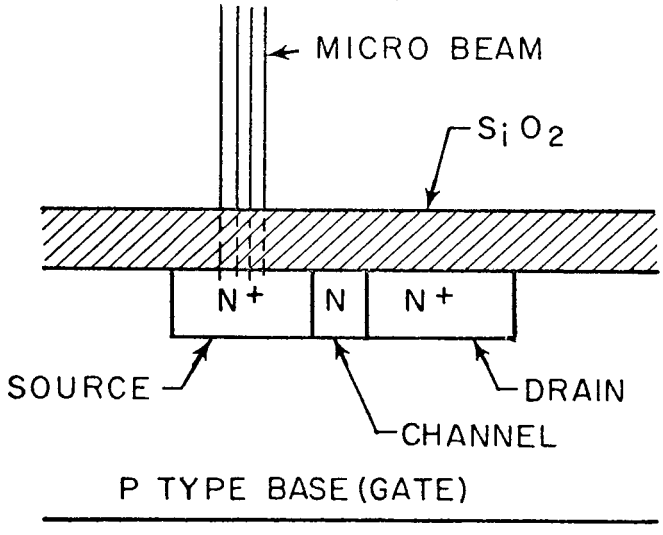

Figure 16. FET Fabrication by Controlled (Maskless) Ion Implantation

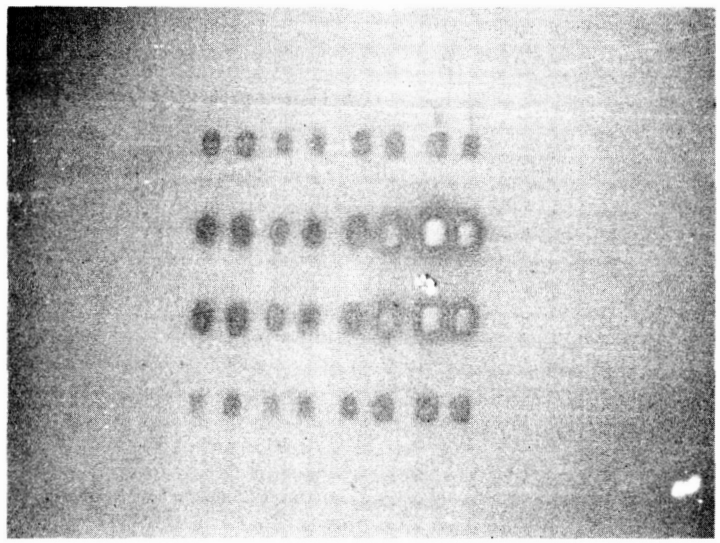

Figure 17. Microbeam "Written" FET Array on Silicon Slice Prior to Annealing (38X)

4. CONCLUSIONS

The future of the microbeam technology must be related to the requirements of device fabrication. For small geometry devices, (less than 0.1 mil) the focused ion beam must be of micron dimension and may require corresponding submicron resolution.

Ion Physics' microbeam equipment is at present, capable of maskless implanting, but technique improvements and equipment development would be required to take commercial advantage of the process.

Normal semiconductor processing requires the success of a great number of successive steps with subsequent loss in yield at each step and involves maintaining the desired resoltuion level at each step. Each diffusion step produces approximately the same doping level at all exposed sites on the slice. This constrains integrated circuit design such that emitter resistors must be doped to the same level as the emitters, etc., or else requires additional diffusion steps.

Ion beam circuit writing techniques eliminate most of these steps and allow freedom to vary doping level from place to place on the slice during the same operation. Concentration, depth, and dopant type can be switched as required while writing the circuit, allowing the freedom to produce such things as buried interconnects, and resistors having identical geometry but with resistances a factor of 1000 apart. Such circuitry can be written at submicron resolution and as many circuits as can be fitted in the field of view of the lens can be written simultaneously. An obvious advantage of the process is the ability to quickly write an experimental circuit.

Beam writing for experimental circuits can be programmed by such techniques as punched tape, curve follower, hand dialing, etc. For production, a tape control or a CRT-mask-photocell, arrangement using parallel scanning of the CRT and ion beam appears to be very useful.

By having greatly reduced the number of steps and by using a process which is inherently more controllable than diffusion, production yields should be greatly improved over those of normal integrated circuit production techniques.

Careful consideration must be given to the methods of registration and contacting to be used. The same requirements that demand small size for speed also creates the need for larger numbers of units on the same substrate. The subsequent multilevel interconnection and long-low resistance paths may be done with the present technology of SiO_2 insulating layers with metalized interconnections. To effectively use this process it must be integrated into

the microbeam system without destroying the flexibility of the system. Using the beam to write a photomask for connection seems to be an attractive solution to part of the problem.

While the ability to "write" many devices simultaneously and fabricate simple devices has been demonstrated, considerable work is required to optimize the technique. Refinements in the microbeam equipment are needed for greater control as detailed in this report.

The exact details of a complete microbeam production line are not predictable from the information available. Ion Physics has developed, built, and is operating a production line for ion implanted solar cells demonstrating the compatibility of ion implantation with production line requirements. The present techniques used for microbeam device fabrication includes steps not suitable as part of a production line. The new techniques developed should have the possibility of being included as part of an automated production line.

The economic factors of device fabrication by this technique have not been explored in significant depth. However, indications are that the implantation step will be economically practical using resolution comparable to present day diffusion technology. Better knowledge of the spherical aberration coefficient of the lens is expected to indicate that implantation at greatly improved resolution can be economically accomplished. With further work should come the information that will allow a realistic economic study to be made. In particular, compatible registration and contacting methods must be developed before an economic appraisal of the system as a whole is made.

Effort is presently directed toward developing devices while maintaining the maximum flexibility of the apparatus with the belief that this flexibility will be the key to use of the microbeam system. The next step in development should result in quality devices and beyond that, simple integrated circuits such as logic gates.

5. REFERENCES

(1) Bond, W. L. and Smits, F. M., BSTJ, 35, 1209 (1956).

(2) Whoriskey, P. J., J. Appl. Phys., 29, 867 (1958).